REPORT DOCUMENTATION PAGE

Form Approved OMB NO. 0704-0188

1. REPORT DATE (DD-MM-YYYY)	2. REPORT TYPE	3. DATES COVERED (From - To)
	New Reprint	-

4. TITLE AND SUBTITLE	5a. CONTRACT NUMBER
Phase and Texture Evolution in Chemically Derived PZT Thin Films on Pt Substrates	W911NF-09-1-0435
	5b. GRANT NUMBER
	5c. PROGRAM ELEMENT NUMBER
	611103

6. AUTHORS	5d. PROJECT NUMBER
Sungwook Mhin, Krishna Nittala, Jinhyung Lee, Douglas S. Robinson, Jon F. Ihlefeld, Geoff L. Brennecka, Luz M. Sanchez, Ronald G. Polcawich, Jacob L. Jones	5e. TASK NUMBER
	5f. WORK UNIT NUMBER

7. PERFORMING ORGANIZATION NAMES AND ADDRESSES	8. PERFORMING ORGANIZATION REPORT NUMBER
University of Florida Office of Engineering 339 Weil Hall Gainesville, FL 32611 -6550	

9. SPONSORING/MONITORING AGENCY NAME(S) AND ADDRESS (ES)	10. SPONSOR/MONITOR'S ACRONYM(S) ARO
U.S. Army Research Office P.O. Box 12211 Research Triangle Park, NC 27709-2211	11. SPONSOR/MONITOR'S REPORT NUMBER(S) 54169-MS-PCS.43

12. DISTRIBUTION AVAILIBILITY STATEMENT

Approved for public release; distribution is unlimited.

13. SUPPLEMENTARY NOTES

The views, opinions and/or findings contained in this report are those of the author(s) and should not contrued as an official Department of the Army position, policy or decision, unless so designated by other documentation.

14. ABSTRACT

The crystallization of lead zirconate titanate (PZT) thin films was evaluated on two different platinum coated Si substrates. One substrate consisted of a Pt coating on a Ti adhesion layer while the other consisted of a Pt coating on a TiO_2 adhesion layer. The Pt deposited on TiO_2 exhibited a higher degree of preferred orientation than the Pt deposited on Ti (as measured by the FWHM of the 111 peak about the sample normal). PZT thin films with a nominal Zr/Ti ratio of 52/48 were deposited on the substrates using the inverted mixing order (IMO) route. Phase and texture evolution of the thin films were monitored during crystallization using in situ X-ray diffraction at a

15. SUBJECT TERMS

ferroelectric, thin film, PZT, in situ characterization

16. SECURITY CLASSIFICATION OF:			17. LIMITATION OF ABSTRACT	15. NUMBER OF PAGES	19a. NAME OF RESPONSIBLE PERSON
a. REPORT	b. ABSTRACT	c. THIS PAGE			Jacob Jones
UU	UU	UU	UU		19b. TELEPHONE NUMBER
					919-515-4557

Standard Form 298 (Rev 8/98)
Prescribed by ANSI Std. Z39.18

Report Title

Phase and Texture Evolution in Chemically Derived PZT Thin Films on Pt Substrates

ABSTRACT

The crystallization of lead zirconate titanate (PZT) thin films was evaluated on two different platinum coated Si substrates. One substrate consisted of a Pt coating on a Ti adhesion layer while the other consisted of a Pt coating on a TiO2 adhesion layer. The Pt deposited on TiO2 exhibited a higher degree of preferred orientation than the Pt deposited on Ti (as measured by the FWHM of the 111 peak about the sample normal). PZT thin films with a nominal Zr/Ti ratio of 52/48 were deposited on the substrates using the inverted mixing order (IMO) route. Phase and texture evolution of the thin films were monitored during crystallization using in situ X-ray diffraction at a synchrotron source. The intensity of the Pt3Pb phase indicated that deposition on a highly oriented Pt/TiO2 substrate resulted in less diffusion of Pb into the substrate relative to films deposited on Pt/Ti. There was also no evidence of the pyrochlore phase influencing texture evolution. The results suggest that PZT nucleates directly on Pt, which explains the observation of a more highly oriented 111 texture of PZT on the Pt/TiO2 substrate than on the Pt/Ti substrate.

REPORT DOCUMENTATION PAGE (SF298)
(Continuation Sheet)

Continuation for Block 13

ARO Report Number   54169.43-MS-PCS
Phase and Texture Evolution in Chemically Deri...

Block 13: Supplementary Note

journal

Phase and Texture Evolution in Chemically Derived PZT Thin Films on Pt Substrates

Sungwook Mhin,[‡] Krishna Nittala,[‡] Jinhyung Lee,[‡] Douglas S. Robinson,[§] Jon F. Ihlefeld,[¶] Geoff L. Brennecka,[¶] Luz M. Sanchez,[∥] Ronald G. Polcawich,[∥] and Jacob L. Jones[‡‡,†]

[‡]Department of Materials Science and Engineering, University of Florida, Gainesville, Florida 32611

[§]Advanced Photon Source, Argonne National Laboratory, Argonne, Illinois 60439

[¶]Electronic, Optical, and Nano Materials Department, Sandia National Laboratories, Albuquerque, New Mexico 87185

[∥]RF MEMS & mm Scale Robotics, U.S. Army Research Laboratory, Adelphi, Maryland 20783

[‡‡]Department of Materials Science and Engineering, North Carolina State University, Raleigh, North Carolina 27695

The crystallization of lead zirconate titanate (PZT) thin films was evaluated on two different platinum-coated Si substrates. One substrate consisted of a Pt coating on a Ti adhesion layer, whereas the other consisted of a Pt coating on a TiO_2 adhesion layer. The Pt deposited on TiO_2 exhibited a higher degree of preferred orientation than the Pt deposited on Ti (as measured by the Full Width at Half Maximum of the 111 peak about the sample normal). PZT thin films with a nominal Zr/Ti ratio of 52/48 were deposited on the substrates using the inverted mixing order (IMO) route. Phase and texture evolution of the thin films were monitored during crystallization using *in situ* X-ray diffraction at a synchrotron source. The intensity of the Pt_3Pb phase indicated that deposition on a highly oriented Pt/ TiO_2 substrate resulted in less diffusion of Pb into the substrate relative to films deposited on Pt/Ti. There was also no evidence of the pyrochlore phase influencing texture evolution. The results suggest that PZT nucleates directly on Pt, which explains the observation of a more highly oriented 111 texture of PZT on the Pt/TiO_2 substrate than on the Pt/Ti substrate.

I. Introduction

L EAD zirconate titanate (PZT) thin films are useful in a number of applications, including microelectromechanical systems (MEMS) and decoupling capacitors.[1–4] PZT compositions near the morphotropic phase boundary (MPB, Zr/ Ti 52/48) are widely used because these compositions exhibit higher piezoelectric coefficients than those further from the MPB.[5] Texture is an important feature of thin films and is defined as a nonrandom distribution of crystallographic orientations.[6] For the purposes of describing different characteristics of the texture in samples used in prior and present work, the following nomenclature is adopted. The texture component is described by planes that are dominantly oriented parallel to the film using the Miller indices in the format *hkl*. A certain fraction of the crystallites in the material may have such an orientation, and this fraction is referred to as the texture fraction. The distribution of these crystallites about the sample normal direction describes the strength or degree of orientation of a particular texture component.

Control of the final texture can allow tailoring of the piezoelectric properties of the thin films.[7] For thin film processing, chemical solution deposition (CSD) has proven effective in being able to control the texture of the film.[8] The substrates selected for use in CSD are an important factor for controlling texture of PZT thin films. For instance, it is reported that Pt thin film coated Si substrates with higher density and stronger 111 texture can provide enhanced 111 textured PZT, thereby improving ferroelectric characteristics.[9] It has also been suggested that improved ferroelectric characteristics result from a decrease in Pb diffusion at the film/Pt interface and templated PZT growth from enhanced 111 textured Pt.[9]

Texture of PZT thin films can also be influenced by altering the processing conditions during crystallization, such as heating rate.[10–12] For example, fast heating rates may result in 111 texture of the thin films on 111 textured Pt substrates.[12] In contrast, slow heating rates for crystallization have been shown to promote 100 texture and/or random orientation in the thin films.[12] Observations such as these suggest that heterogeneous nucleation occurs at the film/ substrate interface during crystallization at fast heating rates, while slow heating rates may promote more homogeneous or randomly oriented nucleation during crystallization.

To explain the texture evolution of PZT thin films on 111 Pt substrates, several mechanisms for the nucleation of 111 texture in the thin films have been proposed.[11–18] Based on the hypothesis that similar lattice parameters between Pt and PZT decrease the activation energy for the formation of PZT, Nittala *et al*. suggested that 111 textured Pt substrates nucleate 111 PZT thin films.[17,18] However, Huang *et al*. suggested that transient 111 Pt_3Pb nucleates 111 PZT during crystallization because the lattice of Pt_3Pb better matches PZT than Pt.[19,20] An alternative theory is that the other common transient phase during crystallization, a pyrochlore/ fluorite phase, transfers its 111 texture to the 111 texture of PZT during crystallization.[21] These results suggest a lack of consensus concerning the proposed mechanism(s) for the nucleation of 111 texture in thin films.

To evaluate the nucleation mechanisms of PZT thin films, it is important to understand the orientation relationship between the resultant PZT and the transient phases that occur during crystallization. The formation of phases and their orientation relationships during crystallization of thin films can be examined using *in situ* X ray diffraction (XRD).[17,18] In the current study, phase and texture evolution of PZT thin films are investigated using *in situ* XRD on two different Pt coated silicon substrates: a commercial Pt/Ti/

SiO₂/Si substrate and a Pt/TiO₂/SiO₂/Si substrate with stronger 111 Pt texture. The influence of strength of texture in the substrates on final texture of the PZT thin films is discussed. Control of texture is also investigated at different heating rates, allowing further insight into the nucleation mechanisms associated with texture selection of PZT thin films.

II. Experimental Procedure

One substrate was a commercial platinized silicon substrate procured from Silicon Quest International (SQI), Santa Clara, CA, and consisted of Pt (170 nm)/Ti (40 nm)/SiO₂ (400 nm)/Si. The SQI sourced substrates were fabricated according to customer specifications by dc sputtering from Ti and Pt metallic targets in an Ar atmosphere without heating the substrate. The second was a textured Pt/TiO₂ coated Si substrate consisting of Pt (100 nm)/TiO₂ (20 nm)/SiO₂ (500 nm)/Si obtained from the U.S. Army Research Laboratory. The processing of the textured Pt/TiO₂ coated Si substrates is described in Potrepka *et al.*[9] In this process, a highly *0001* textured Ti layer is sputtered at room temperature onto a SiO₂ coated Si substrate. Next, the Ti layer is converted into a highly 100 textured TiO₂ layer through a 750°C anneal in an oxygen environment. Finally, 111 textured Pt is sputtered onto the TiO₂ at 500°C.

PZT thin film samples were prepared using 0.35*M* solution derived Pb(Zr₀.₅₂Ti₀.₄₈)O₃ with 20% Pb excess through the inverted mixing order (IMO) method detailed by Schwartz *et al.*[22] The dispensed PZT solution was spin cast for 30 s at 3000 rpm on two different square sections of the platinized silicon substrates. Pyrolysis of the PZT thin films was completed on a hotplate for 1 min either at 300°C for the Pt/Ti coated substrates or 350°C for the PZT on the textured Pt/TiO₂ coated substrates. The spin coating and pyrolysis sequence were repeated twice more, for a total of three pyrolysis treatments per sample to achieve a thickness of 250 nm after crystallization. The hotplate temperature was monitored using an external IR laser digital thermometer (HDE B01; HDE, Allentown, PA).

In situ XRD experiments were conducted using synchrotron X ray beamline 6 ID B at the Advanced Photon Source, Argonne National Laboratory. The wavelength of the synchrotron X ray is 0.546186 Å. A graphic representation of the *in situ* XRD geometry is shown in Fig. 1(a). A low incidence angle (~0.5°) of the X ray beam was used to maximize the interaction volume in the thin films. XRD patterns of thin films during heating were recorded in a 2D detector. The thin films were crystallized during heating at different rates with the heating rates controlled by applying a voltage on an IR lamp. The voltage was controlled using a digital to analog converter program providing a voltage signal between 0 V

and 5 V to a solid state power controller (Control Concepts Inc. 1032 A, Chanhassen, MN). This measurement setup has been discussed in detail and used in prior work.[17,18]

Representative XRD patterns recorded in the 2D detector are shown in Fig. 1(b). The patterns are referenced by azimuthal angle (γ) and radial distance (r). The radial distance (r) from the beam center on the 2D detector is directly related to the 2θ angle and the sample to detector distance (D) through the following relation:

$$\tan 2\theta = r/D. \tag{1}$$

Data reduction of the XRD patterns was conducted for phase and texture analysis with different radial distance (r) and azimuthal angles (γ).[23] For example, diffraction intensities versus 2θ over the γ range in Section I [Fig. 1(b)] can be integrated. The collection of the integrated diffraction intensities during heating can be plotted as a function of 2θ and temperature. This representation is referred to as a phase evolution plot, an example of which is given in the left hand side of Fig. 2. Also, the intensities of *hkl* reflections in Section II [Fig. 1(b)] can be integrated through 2θ over the γ range. The collection of the integrated diffraction intensities during heating can be plotted as a function of γ and temperature. This representation is referred to as a texture evolution plot, as shown in the center column of Fig. 2.

Temperature profiles during *in situ* measurements were determined from the coefficient of thermal expansion (CTE) of an internal standard in an additional set of measurements. Details of the temperature calibration are described in previous work.[18] The temperature profiles are shown in parallel with the phase and texture evolution plots in Fig. 2. T_{CTE} in the figure refers to the temperature determined via this approach. The corresponding average heating rates for the different voltage rates used for the *in situ* XRD measurements are also shown in the figure.

Integrated intensities and the Full Width at Half Maximum (FWHM) of the intensity of the *hkl* texture components in PZT were extracted from the texture evolution plots in Fig. 2 (center panel). The Pearson VII profile shape function was used to fit the measured intensities and extract quantitative information about the component texture fractions and strengths. Background intensities were modeled using a linear polynomial function. The background intensities correspond to both conventional background scattering and diffraction intensities from randomly oriented grains. The texture fraction of a given texture component *hkl* can be calculated using the integrated intensity and the multiplicities of the pseudo cubic {110} reflections, as described in Refs. [17] and [18]. Further details of the *in situ* synchrotron X ray
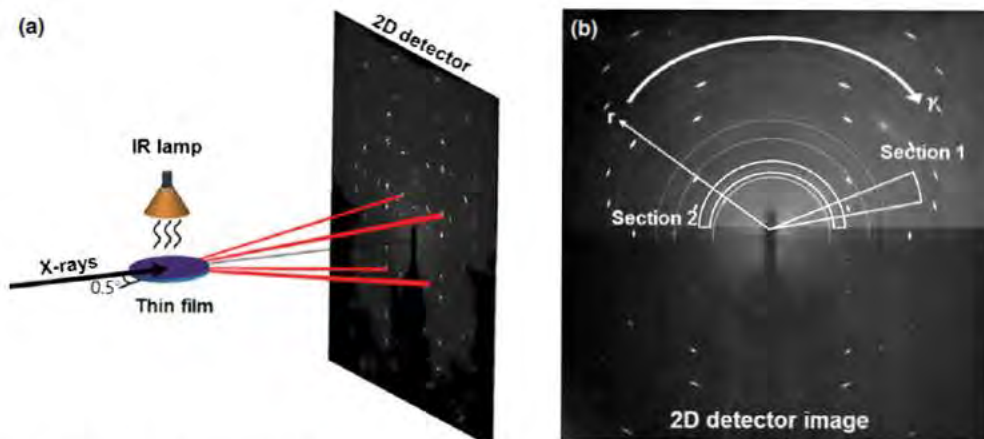

Fig. 1. (a) Schematic diagram of the experimental geometry used on beamline 6 ID B for *in situ* crystallization of lead zirconate titanate thin films, and (b) representative 2D detector image.
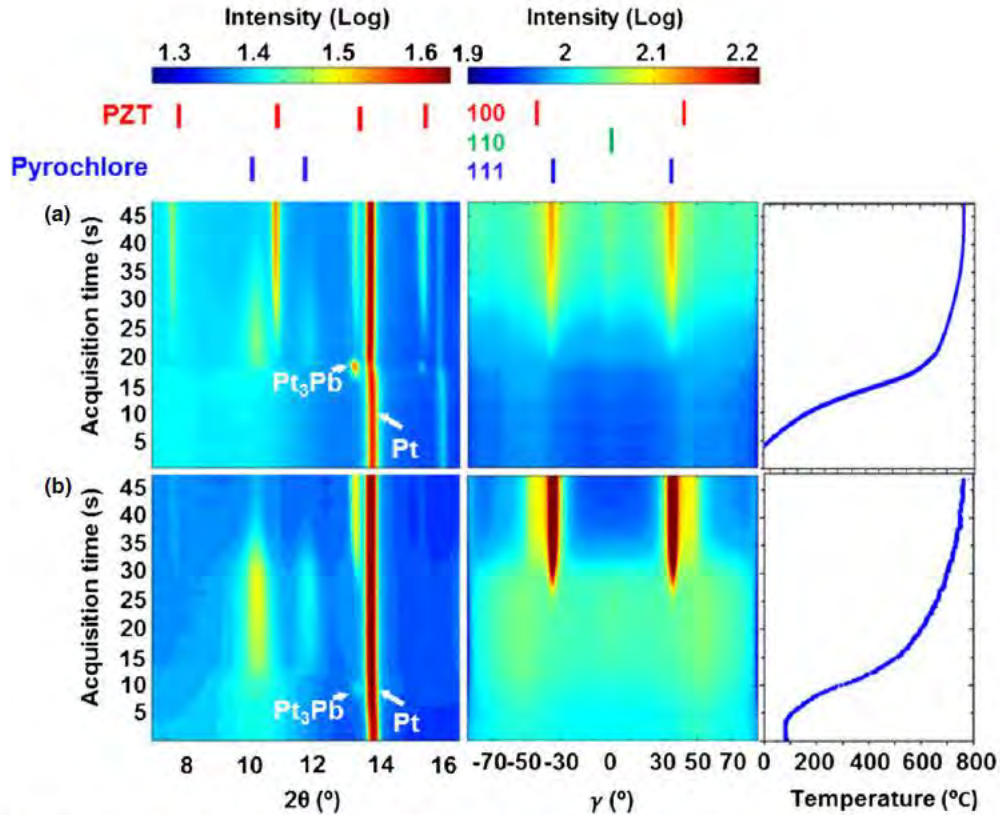
Fig. 2. Phase (left panel) and texture evolution (center panel) plots of PZT thin films on Pt substrates: (a) Pt/Ti coated substrate, and (b) Pt/TiO$_2$ coated substrate.

measurements and data analysis that are used here have been described in Nittala *et al.*[17,18]

III. Results and Discussion

The differences between the textures of the initial Pt substrates are discussed first. The initial texture of the Pt substrates is shown using the intensity of the 111 Debye Scherrer ring as a function of azimuthal angle. These data are extracted from the initial images of both substrates and are shown in Fig. 3(a). Peaks in diffracted 111 intensity were observed at angles of $\gamma \approx 72°$, 0°, and 72° from both Pt substrates. A low 111 diffracted intensity measured at $\gamma \approx 0°$ for the textured Pt/TiO$_2$ coated Si substrates is because the scattering geometry does not measure planes perfectly parallel to the thin films.[18] In this diffraction geometry that employs a 2D area detector, the diffracted intensity of 111 texture components from a strong 111 Pt substrate may be decreased in the near vertical direction of the 2D detector ($\gamma \approx 90°$).[18] The measurements shown in Fig. 3(a) are similar, but not equivalent, to a rocking curve over a large angular range. An obvious difference between these intensity distributions from the two substrates before heating is that the FWHM of the peak from the textured Pt/TiO$_2$ coated substrates (2.7°) is narrower than that in the Pt/Ti substrates (5.2°). This difference in the strength of 111 Pt texture is evidence that the Pt/TiO$_2$ coated substrates have a stronger texture than that of the Pt/Ti coated substrates.

Representative XRD patterns of the PZT thin films after crystallization are shown in Fig. 3(b) for both Pt substrates. XRD patterns show that the films consist of a phase pure pseudo cubic (PC) perovskite. A major difference between the XRD patterns from the films on the two substrates is that the intensity of the {111}$_{PC}$ profile (consisting of any or all (111) reflections from perovskite phase(s)) is higher in the film crystallized on the textured Pt/TiO$_2$ coated Si substrate. This demonstrates a correlation between the 111 Pt texture

strength of the Pt/TiO$_2$ coated substrates and the resulting texture of the PZT thin film, a result that is consistent with prior work.[9]

To investigate the phase evolution during crystallization of PZT thin films, representative XRD patterns of the thin films during heating are shown on the left hand side of Fig. 2. The data show reflections ($7° \leq 2\theta \leq 17°$) between $\gamma \approx 70°$ and 80° on the detector that correspond to scattering vectors that are ~70° from the normal to the film. The peak positions corresponding to the PZT and pyrochlore phase are indicated using tick marks above the figure. A similar sequence in the phase evolution is observed in the thin films on both substrates as shown on the left hand side of Fig. 2. The thin films are initially amorphous. During heating, the intermetallic Pt$_3$Pb phase was the first phase to be observed in both films. (Note the difference in intensity of this peak between the two films, which is discussed later) The Pt$_3$Pb phase disappeared in conjunction with the formation of a pyrochlore phase. Finally, perovskite PZT phase was observed with the disappearance of the pyrochlore phase.

The formation of an intermetallic Pt$_3$Pb phase has been proposed due to Pb diffusion from amorphous PZT thin films into the Pt substrate.[17,19,20] During crystallization of the thin films, the elimination of organic compounds leads to the formation of local reducing conditions at the Pt/film interface.[17,18] These local reducing conditions allow the reduction of the Pb precursor (Pb^{2+}) in the thin films to metallic Pb (Pb^0).[18,24] The metallic Pb diffuses into the Pt substrate, forming the Pt$_3$Pb phase. The extent of the local reducing conditions depends on the combustion of precursor organics as well as the extent of oxygen diffusion from the surroundings to the Pt/film interface.[24,25] In Fig. 2, Pt$_3$Pb was observed during the crystallization of PZT thin films on both Pt substrates. However, the maximum intensity of (111) Pt$_3$Pb on the Pt/TiO$_2$ coated substrate is weaker than that on the Pt/Ti coated substrate. This observation may indicate that the high density Pt on the Pt/TiO$_2$ coated substrate is
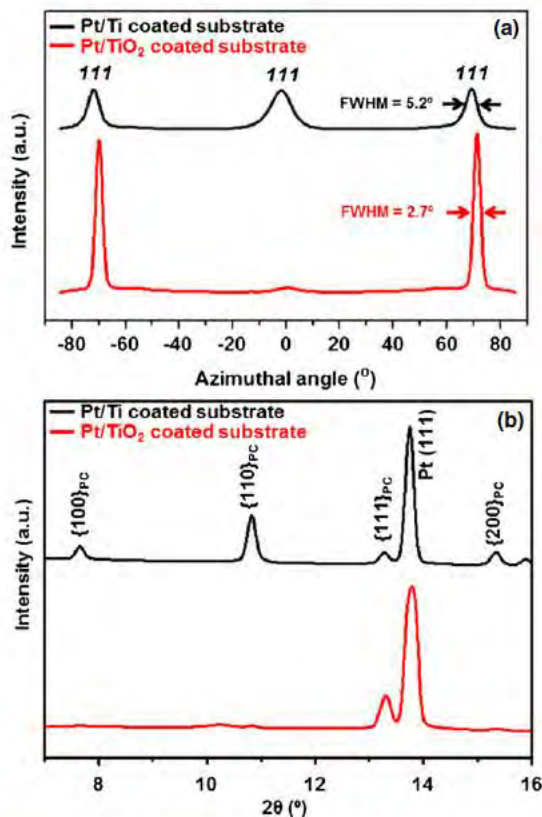
Fig. 3. (a) Azimuthal angle intensity plot of Pt substrates, and (b) XRD patterns of lead zirconate titanate thin films on Pt substrates after crystallization. PC refers to pseudo cubic crystal structure.
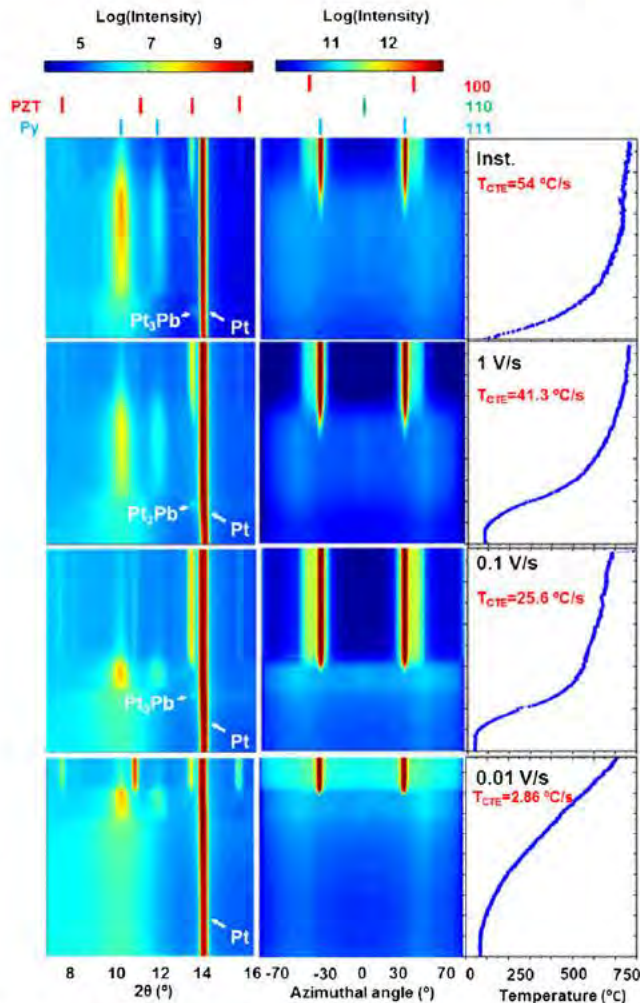

Fig. 4. Phase (left panel) and texture (center panel) evolution plots of lead zirconate titanate thin films on Pt/TiO$_2$ coated substrates at different heating rates (right panel). The vertical direction for each panel is acquisition time and each plot uses an independent time scales. (Instantaneous heating is represented as Inst.).

effective in limiting the diffusion of Pb from the thin films into the Pt layer and minimizes accumulation along easy diffusion pathways such as grain boundaries and pores.[9]

Another hypothesis for the formation of less Pt$_3$Pb in the Pt/TiO$_2$ coated substrate is that there is less reduction of elemental Pb from the amorphous PZT layer because a fully oxidized TiO$_2$ adhesion layer would not deplete oxygen from the amorphous PZT during heating, resulting in less reducing conditions at the Pt/film interface. This may reduce the diffusion of Pb from the amorphous layer into the Pt substrate. Phase evolution of PZT thin films on Pt/TiO$_2$ coated substrates at different heating rates is shown in Fig. 4 (left panel). The intensity of the (111) reflections of Pt$_3$Pb on Pt/TiO$_2$ coated substrates was found to decrease with decreasing heating rates (Fig. 4). This suggests that more oxygen can diffuse into the Pt/film interface at slower heating rates to compensate for the loss of oxygen during the removal of organic compounds.[17] In a previous study, a decrease in intensity of the (111) reflections of Pt$_3$Pb with decreasing heating rates was also observed on similar Pt/Ti coated substrates.[17]

111 textured Pt substrates have been suggested to promote 111 texture of the Pt$_3$Pb phase during crystallization of PZT thin films.[18] To investigate the orientation relationship between Pt and Pt$_3$Pb, the reflections of Pt and Pt$_3$Pb over the γ range were extracted. The azimuthal angle 2θ plot of the Pt$_3$Pb and Pt is presented in Fig. 5 for the time during the experiment when the intensity of Pt$_3$Pb is at its maximum value. Similar nonuniform intensity distribution is observed in the 111 Debye Scherrer rings of Pt and Pt$_3$Pb. For example, the diffraction intensity from both the 111 Pt and 111 Pt$_3$Pb is present at the γ angles of 72°, 0°, and 72° near the 2θ range ~13.5°. An extension of this idea to other *hkl* reflections results in a similar observation, that is, that there is an orientation relationship between Pt$_3$Pb and Pt.

The transient 111 Pt$_3$Pb was also previously suggested to promote 111 texture of PZT thin films due to good lattice matching.[17,19,20] If 111 texture in PZT is nucleated by 111 Pt$_3$Pb, then the diffraction intensities of these two phases should overlap during heating. However, as observed in Fig. 6, there is no coexistence of the (111) reflection of Pt$_3$Pb and the (111) reflection of PZT on either of the Pt substrates. It is assumed that Pt$_3$Pb disappears completely when there is no intensity observed in the XRD patterns. The 111 PZT forms after the disappearance of the 111 Pt$_3$Pb and, as a result, it can be inferred that the 111 Pt$_3$Pb does not nucleate 111 PZT.[18] As the intermetallic disappears, lead (or lead oxide) from the Pt$_3$Pb could be incorporated into the pyrochlore phase of the film or the Pt substrates, as discussed in Ref. [17]. The lack of overlap between PZT and Pt$_3$Pb reflections is observed at all heating rates [Fig. 4 (left panel)]. Thus, there is no evidence that a 111 textured Pt$_3$Pb influences the formation of 111 PZT thin films.

Given the observation that 111 oriented nuclei of Pt$_3$Pb do not provide nucleation sites for 111 oriented PZT, a second hypothesis introduced earlier involving the possibility of an intermediate pyrochlore phase promoting 111 textured PZT is now considered and discussed. To investigate the texture of the pyrochlore phase, the intensity distribution of the (222) reflection of the pyrochlore phase ($10.6° \leq 2\theta \leq 11.4°$) is shown in Fig. 7. It has been suggested that the formation of the pyrochlore phase from amorphous PZT occurs prior to the formation of perovskite PZT due to easier atomic rearrangement with lower energy.[26] Preferred orientation of
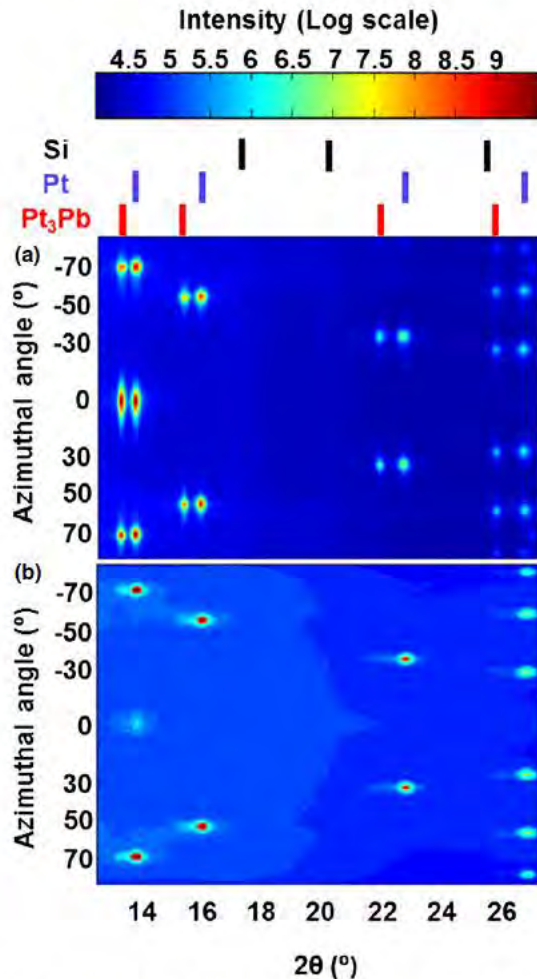
Fig. 5. Azimuthal angle 2θ plot of Pt3Pb and Pt at the maximum peak intensity during crystallization: (a) Pt/Ti coated substrate, and (b) Pt/TiO₂ coated substrate.

Fig. 6. Phase evolution plots of (111) Pt3Pb and (111) lead zirconate titanate during crystallization: (a) Pt/Ti coated substrate, and (b) Pt/TiO₂ coated substrate.

Fig. 7. Texture of the pyrochlore phases prior to the formation of lead zirconate titanate.

the pyrochlore phase is suggested to influence the final texture of PZT thin films. For example, Norga *et al.* proposed that 111 textured pyrochlore phase is nucleated by the Pt substrate.[21] The 111-textured pyrochlore phase is said to transform to perovskite PZT while maintaining an orientation relationship with the Pt substrate.[21] A broad and weak intensity distribution of the (222) reflection of the pyrochlore phase over the γ range was observed prior to the formation of perovskite PZT thin films on both substrates, which implies that the pyrochlore phase is almost randomly oriented prior to the formation of PZT thin films. It is therefore likely that the pyrochlore phase is not heterogeneously nucleated at the Pt/film interface. Thus, there is no evidence from this study that a 111 textured pyrochlore promotes 111 texture of PZT thin films.

In prior work, it was determined that the texture selection in IMO derived PZT thin films on Pt/Ti coated substrates was strongly affected by the heating rate.[17] To understand the formation of texture in PZT thin films deposited on Pt/TiO₂ coated substrates, (110)$_{PC}$ PZT reflections (10.6° ≤ 2θ ≤ 11.4°) over the γ range during heating are shown in Fig. 4 (center panel). Tick marks above indicate the positions of peaks corresponding to different types of possible PZT textures. In the films, diffracted intensity from the 111 PZT texture component was observed prior to the 100 texture component during heating. In addition, strong 111 texture with weak intensity of 100 texture was observed in fully crystallized films. However, the texture selection in the thin films also strongly depends on heating rates during crystallization, as shown in the center panel of Fig. 4: a dominant 111
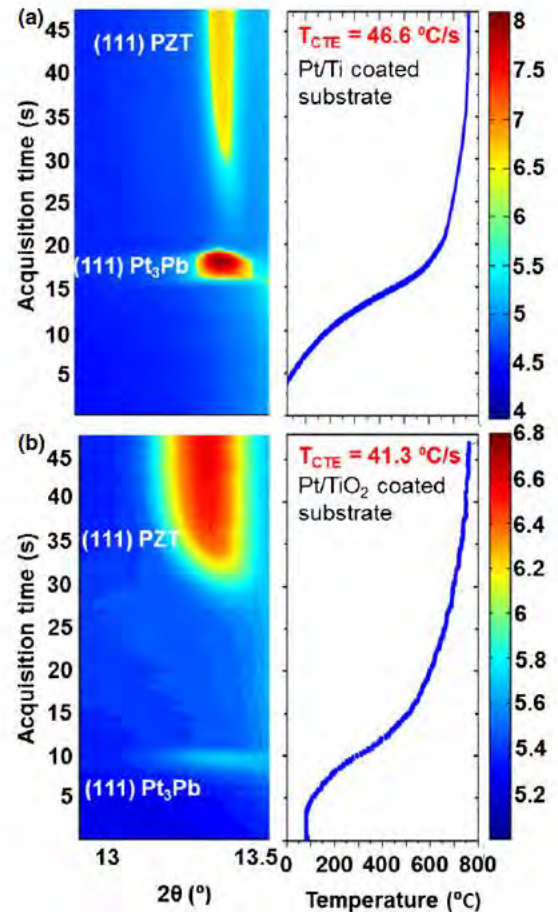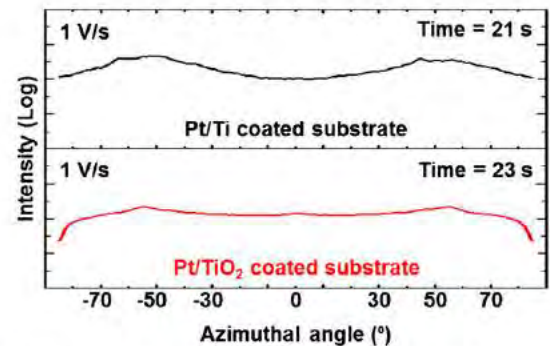
texture was observed at faster heating rates, whereas a 111 texture with ***random*** components was observed at slower heating rates. This implies that a dominant heterogeneous nucleation of 111 PZT texture occurs at faster heating rates.

Quantitative assessment of the diffraction patterns can provide further insight into the mechanisms associated with texture selection of PZT thin films. Nittala *et al.* demonstrated this to understand the nucleation mechanisms using both FWHM and the texture fraction of IMO derived thin films on Pt/Ti coated substrates.[17,18] It was suggested that a 111 Pt coated substrate can provide energetically favorable nucleation sites and decrease the nucleation energy, promoting the formation of 111 texture in PZT thin films.[17] In the present work, the final FWHM and different types of texture components are shown in Fig. 8 as a function of heating rate. The FWHM of the 111 PZT texture components is sim
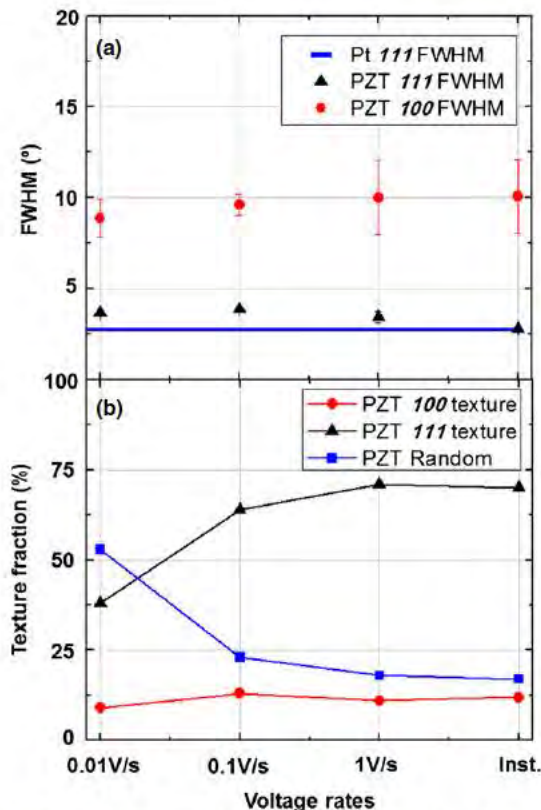
Fig. 8. (a) Full Width at Half Maximum (FWHM) of the 100 and 111 texture components of lead zirconate titanate thin films at the maximum temperature during crystallization and FWHM of 111 texture components in Pt/TiO₂ coated substrate prior to the crystallization, and (b) Texture fraction of different texture components at different voltage rates at the maximum temperature during crystallization (Instantaneous heating is represented as Inst.).

factors to increasing the 111 texture strength and fraction of PZT thin films.[17]

IV. Conclusions

Chemical solution deposition using the IMO method was used to prepare PZT thin films on two Pt coated Si substrates: one using a Pt/Ti coating with a broader Pt (111) FWHM, and the other using a Pt/TiO₂ coating with a narrower Pt (111) FWHM. Phase and texture evolution of PZT thin films during heating at different rates were investigated using *in situ* synchrotron XRD. During heating, less diffusion of Pb into Pt occurred from the thin films crystallized on Pt/TiO₂, evidenced by lower intensity of the (111) reflection in the transient Pt₃Pb phase. Also, stronger 111 PZT texture was observed in films crystallized on Pt/TiO₂ versus Pt/Ti. In addition, faster heating rates during crystallization are found to be effective to enhance 111 textured PZT. There is no evidence that Pt₃Pb and pyrochlore phases nucleate 111 PZT during heating. The results support the theory that 111 texture of the thin films may be nucleated directly from 111 Pt substrates. It is concluded that stronger 111 textured Pt substrates play an important role in synthesizing strongly 111 oriented PZT thin films.

ilar in Pt/TiO₂ coated substrates at all heating rates. Moreover, the FWHM values are similar to those of the 111 Pt substrates. The results support that 111 PZT texture of the thin films is derived via templated growth from the 111 oriented Pt.[17] In contrast, the FWHM of 100 PZT texture components is much broader than the 111 PZT texture components at all heating rates and is approximately 10° for the fastest heating rate. It was also observed that the FWHM of the 100 texture component slightly decreases with a decrease in the heating rate.

In the PZT thin films on Pt/TiO₂ coated substrates, as shown in Fig. 8(b), the fraction of 111 PZT texture increased with increasing heating rates, which implies that faster heating rates may enable heterogeneous nucleation of the 111 PZT orientations on 111 Pt substrates. Conversely, the fraction of *random* components increased with decreasing heating rates. In previous work on Pt/Ti coated substrates, the 100 texture components also increased at slower heating rates.[17] In contrast, however, the present work shows that the fraction of 100 PZT texture components on the Pt/TiO₂ coated substrate is not a strong function of heating rate. In the present work, the inverse correlation between the fraction of random and 111 PZT texture components suggests a balance between preferential (111) nucleation and randomly oriented nucleation.[18] The present results show that the heating rate is a useful variable that can be used to control this balance. The magnitude of 111 texture fraction observed in Pt/TiO₂ coated substrates (74%, as shown in Fig. 8) is also substantially larger relative to that observed on Pt/Ti coated substrates (50%, as shown in Ref. 17). The results from Fig. 8 therefore provide further evidence that substrate texture strength and fraction are key

References

[1]P. Muralt, R. G. Polcawich, and S. Trolier-McKinstry, "Piezoelectric Thin Films for Sensors, Actuators, and Energy Harvesting," *MRS Bull.*, **34**, 658 64 (2009).
[2]P. Muralt, "Recent Progress in Materials Issues for Piezoelectric MEMS," *J. Am. Ceram. Soc.*, **91**, 1385 96 (2008).
[3]S. Tadigadapa and K. Mateti, "Piezoelectric MEMS Sensors: State-of-the-Art and Perspectives," *Meas. Sci. Technol.*, **20**, 092001, 30pp (2009).
[4]R. G. Polcawich and J. S. Pulskamp, "Piezoelectric MEMS"; pp. 273 344 in *MEMS Materials and Processes Handbook*, Vol. **1**, 1st edn., Edited by R. Ghodssi and P. Lin. Springer, New York, NY, 2011.
[5]S. Trolier-McKinstry and P. Muralt, "Thin Film Piezoelectrics for MEMS," *J. Electroceram.*, **12**, 7 17 (2004).
[6]U. F. Kocks, *Texture and Anisotropy: Preferred Orientations in Polycrystals and Their Effect on Materials Properties.* p. 676. Cambridge University Press, Cambridge, 2000.
[7]F. Calame, "PZT Thin Film Growth and Chemical Composition Control on Flat and Novel Three-dimensional Micromachined Structures for MEMS Devices"; Ph.D dissertation, École Polytechnique Fédérale De Lausanne, Lausanne, Switzerland, 2007.
[8]L. Sanchez, D. Potrepka, G. Fox, I. Takeuchi, and R. G. Polcawich, "Optimization of PbTiO₃ Seed Layers and Pt Metallization for PZT Based PiezoMEMS Actuators," *J. Materials Res.*, **28**, 1920 31 (2013).
[9]D. M. Potrepka, G. R. Fox, L. M. Sanchez, and R. G. Polcawich, "Pt/TiO₂ Growth Templates for Enhanced PZT films and MEMS devices"; MRS Online Proc. Library, Material Research Society, 1299, mrsf10-1299 s04-02, 2011.
[10]G. L. Brennecka, J. F. Ihlefeld, J. P. Maria, B. A. Tuttle, and P. G. Clem, "Processing Technologies for High-Permittivity Thin Films in Capacitor Applications," *J. Am. Ceram. Soc.*, **93**, 3935 54 (2010).
[11]K. G. Brooks, I. M. Reaney, R. Klissurska, Y. Huang, L. Bursill, and N. Setter, "Orientation of Rapid Thermally Annealed Lead Zirconate Titanate Thin Films on (111) Pt Substrates," *J. Mater. Res.*, **9**, 2540 53 (1994).
[12]S. Y. Chen and I. W. Chen, "Temperature-Time Texture Transition of Pb(Zr₁ ₓTiₓ)O₃ Thin-Films: II. Heat-Treatment and Compositional Effects," *J. Am. Ceram. Soc.*, **77**, 2337 44 (1994).
[13]S. Y. Chen and I. W. Chen, "Temperature-Time Texture Transition of Pb(Zr₁ ₓTiₓ)O₃ Thin-Films: I. Role of Pb-Rich Intermediate Phases," *J. Am. Ceram. Soc.*, **77**, 2332 6 (1994).

[14]P. Muralt, "Texture Control and Seeded Nucleation of Nanosize Structures of Ferroelectric Thin Films," *J. Appl. Phys.*, **100**, 051605 16 (2006).

[15]P. Muralt, T. Maeder, L. Sagalowicz, S. Hiboux, S. Scalese, D. Naumovic, R. G. Agostino, N. Xanthopoulos, H. J. Mathieu, L. Patthey, and E. L. Bullock, "Texture Control of PbTiO$_3$ and PZT Thin Films with TiO$_2$ Seeding," *J. Appl. Phys.*, **83**, 3835 41 (1998).

[16]S. Y. Chen and I. W. Chen, "Texture Development, Microstructure Evolution, and Crystallization of Chemically Derived PZT Thin Films," *J. Am. Ceram. Soc.*, **81**, 97 105 (1998).

[17]K. Nittala, S. Mhin, K. M. Dunnigan, D. S. Robinson, J. F. Ihlefeld, P. G. Kotula, G. L. Brennecka, and J. L. Jones, "Phase and Texture Evolution in Solution Deposited Lead Zirconate Titanate Thin Films: Formation and Role of the Pt$_3$Pb Intermetallic Phase," *J. Appl. Phys.*, **113**, 244101, 11pp (2013).

[18]K. Nittala, S. Mhin, J. L. Jones, D. S. Robinson, J. F. Ihlefeld, and G. L. Brennecka, "*In situ* X-ray Diffraction of Solution-Derived Ferroelectric Thin Films for Quantitative Phase and Texture Evolution Measurement," *J. Appl. Phys.*, **112**, 104109, 10pp (2012).

[19]Z. Huang, Q. Zhang, and R. W. Whatmore, "The Role of an Intermetallic Phase on the Crystallization of Lead Zirconate Titanate in Sol gel Process," *J. Mat. Sci. Lett.*, **17**, 1157 9 (1998).

[20]Z. Huang, Q. Zhang, and R. W. Whatmore, "Low Temperature Crystallization of Lead Zirconate Titanate Thin Films by a Sol-Gel Method," *J. Appl. Phys.*, **85**, 7355 61 (1999).

[21]G. J. Norga, F. Vasiliu, L. Fe, D. J. Wouters, and O. Van der Biest, "Role of Fluorite Phase Formation in the Texture Selection of Sol-Gel-Prepared Pb(Zr$_{1-x}$, Ti$_x$)O$_3$ Films on Pt Electrode Layers," *J. Mater. Res.*, **18**, 1232 8 (2003).

[22]R. A. Assink and W. Schwartz, "Chemical Solution Deposition of Perovskite Thin Films," *Chem. Mater.*, **5**, 511 7 (1993).

[23]B. B. He, *Two-Dimensional X-Ray Diffraction*. p. 426. John Wiley & Sons, Inc., New Jersey, NJ, 2009.

[24]L. A. Bursill and K. G. Brooks, "Crystallization of Sol-Gel Derived Lead-Zirconate-Titanate Thin Films in Argon and Oxygen Atmospheres," *J. Appl. Phys.*, **75**, 4501 9 (1994).

[25]S. Mhin, C. Cozzan, K. Nittala, P. Wanninkhof, J. F. Ihlefeld, G. L. Brennecka, and J. L. Jones, "Effect of Switching Atmospheric Conditions during Crystallization on the Phase Evolution of Solution-Derived Lead Zirconate Titanate Thin Films," *J. Am. Ceram. Soc.*, **96**, 2706 9 (2013).

[26]C. K. Kwok and S. B. Desu, "Formation Kinetics of PbZr$_x$Ti$_{1-x}$O$_3$ Thin Films," *J. Mater. Res.*, **9** [7] 1728 33 (1994).   □